Electronic Supporting Information for "**Reversible de-/resolvation and accompanied magnetism modulation in a framework of topologically ferrimagnetic $[Co_3(\mu_3\text{-}OH)_2]_n$ chains linked by V-shaped ligand 4,4´-dicarboxybiphenyl sulfone**" by W. J. Zhuang *et al.*.

1. Synthesis

All starting chemicals were commercially available, reagent grade, and used without further purification.

Synthesis of **1**: A mixture of $CoCl_2 \cdot 6H_2O$ (0.48 g, 2.0 mmol), H_2*dbsf* (0.60 g, 2.0 mmol), water (40 mL), ethanol (40 mL) and N,N-dimethylformamide (2 mL) was sealed in a Teflon-lined stainless vessel (120 mL) and heated at 160°C for 72 h under autogenous pressure. Pink long-plate-shaped crystals were obtained. Yield: 0.42 g (44%). Anal. calcd. for $C_{31}H_{35}Co_3O_{19.5}S_2$: C 38.76, H 3.67%; found: C 38.74, H 3.76%.

Synthesis of **2**: Crystals of **2** were obtained by heating the crystals of **1** at 50°C under dynamic vacuum (10^{-2} torr) for 12 hours and after that period constant weight of the sample was achieved. The weight loss of the sample was 15.4% *vs.* the calcd. 14.7%. The crystals became finely cracked, and the color changed from pink to blue. Anal. (%), calcd. for $C_{28}H_{18}Co_3O_{14}S_2$: C 41.05, H 2.21%; found: C 40.37, H 2.85%.

Sample of the resolvated **2** was obtained by directly adding an ethanol-water mixed solvents with v:v ratio of 1:1 in the vessel containing **2.** The color of sample changed from blue to pink within one minute after the addition of the solvents (see Fig. S4). The sample was immersed in the solvents for 30 minutes, and the solution kept colorless. After the solvents were removed, the pink resolvated sample was washed by ethanol three times, and dried in vacuum. The mass gain upon resolvation is 14.9%, closed to the calculated 14.7%. Anal. calcd. for $C_{31}H_{35}Co_3O_{19.5}S_2$: C 38.76, H 3.67%; found: C 39.22, H 3.78%. The crystals seemly become further cracked after resolvation. The thermal analysis, IR and PXRD (see Fig. S2 to S5) together with above element analysis results for the sample of the resolvated **2,** confirmed that the resolvation of **2** recovered **1**.

2. X-ray crystallography and physical measurements

The crystallographic data for the single crystal of **1** were collected at room temperature on a Bruker SMART 1000 CCD diffractometer using graphite monochromated Mo Kα radiation (λ = 0.71073 Å). The structure was solved by direct method and refined by full-matrix least-squares on F^2 using SHELX program. The H atoms of the framework and coordination water and ethanol molecules were added according to the ideal geometry and not refined, but not added for the disordered lattice water and ethanol. CCDC-764743 contains the supplementary crystallographic data of **1**. These data can be obtained free of charge via www.ccdc.cam.ac.uk/conts/retrieving.html (or from the Cambridge Crystallographic Data Centre, 12 Union Road, Cambridge CB2 1EZ, UK; fax: (+44) 1223-336-033; or e-mail: deposit@ccdc.cam.ac.uk).

Several carefully selected crystals of **2** were subjected to single crystal X-ray diffraction experiments on a Nonius KappaCCD diffractometer, in order to determine the structure. Unfortunately, the finely cracked crystals showed very high mosaicity and low diffraction ability, thus hindered the structure determination, though several data sets were collected. However, the lattice type and the unit cell parameters could be fairly obtained by these data sets, as described in text.

Powder X-ray diffraction (PXRD) data for **1**, **2** and resolvated **2** were collected in the range of $5° < 2\theta < 55°$ at room temperature against the bulk samples on a X'Pert PRO MPD X-Ray diffractometer or a Rigaku Rint 2000 diffractometer with Cu Kα radiation in a flat plate geometry. The experimental PXRD pattern of **1** matched well the calculated one from the single-crystal structures (Fig. S3b), confirming the phase purity of the bulk sample. The PXRD pattern of the resolvated **2** featured those of **1**, indicating the recovery of **1** by resolvation of **2**.

Element analysis of carbon and hydrogen were performed on an Elementar Vario EL or an Elementar Vario MICRO CUBE analyzer. FTIR spectra were recorded against pure samples of **1** and **2** on a Nicolet Magna 750 FT/IR spectrometer and resolvated **2** on a NICOLET iN10 MX spectrometer in the range of 4000 to 650 cm^{-1}. UV-Vis spectra of **1** and **2** were recorded on a SHIMADZU UV-VIS-3100 spectrophotometer with an integrated sphere attachment in the range 200 to 800 nm on ground powder samples referenced to a $BaSO_4$ background. Thermal analyses, TGA and DTA, were performed at the rate

of 5°C/min under air, on a SDT 2960 thermal analyzer for **1** and **2**, and on a SDT Q600 for the resolvated **2**. Magnetic measurements were performed for **1** and **2** on a Quantum Design MPMSXL5 SQUID system with samples tightly packed and sealed in a capsule. Diamagnetic corrections were estimated using Pascal constants and background correction by experimental measurement on sample holders.

3. Figures

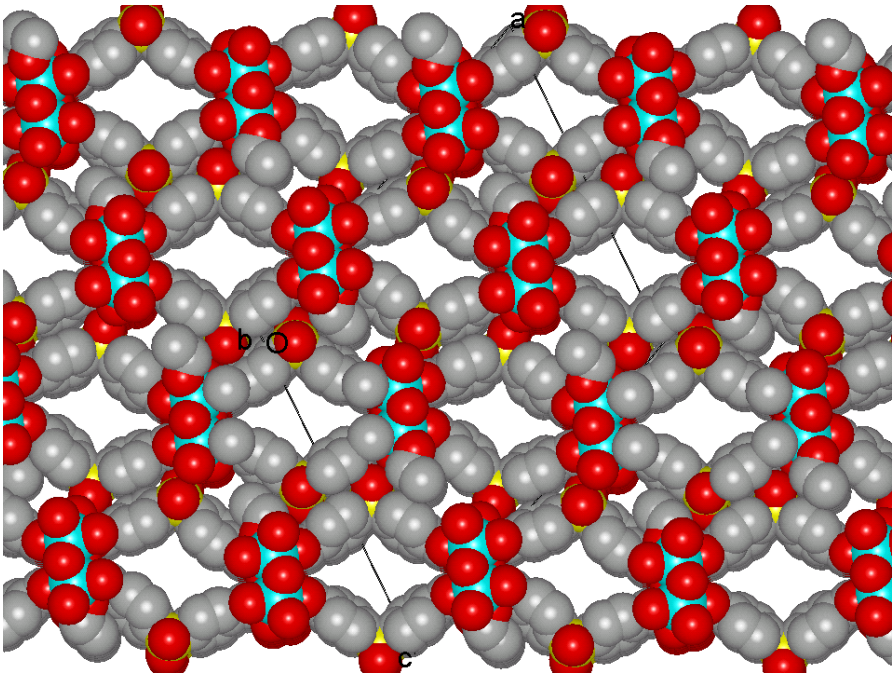

Fig. S1. Space filling plot of the framework structure of **1**, with the same view direction and atomic scheme as Fig. 1b. H-atoms and lattice solvents within the channels are omitted for clarity.

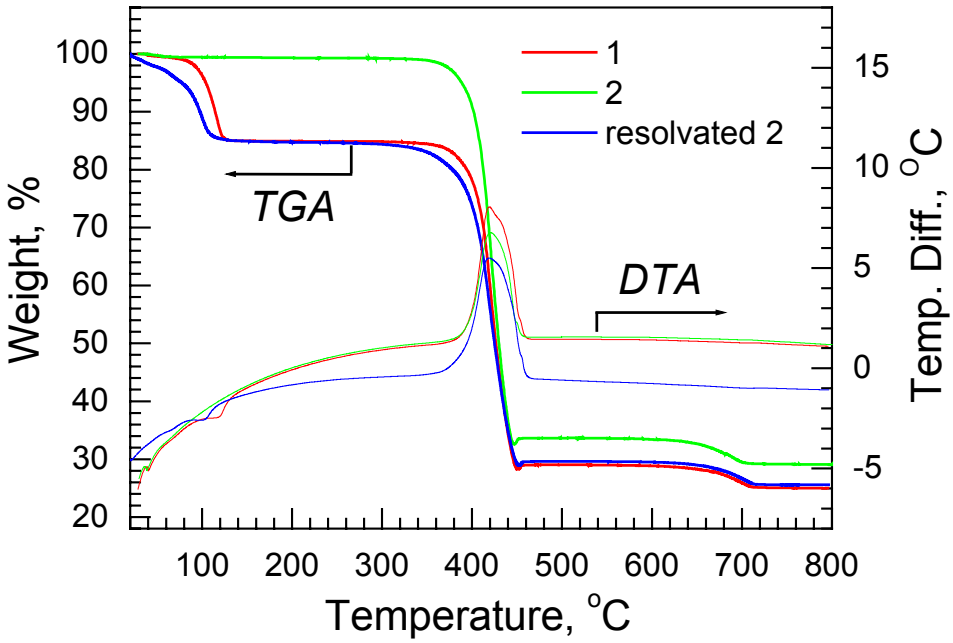

Fig. S2. TGA/DTA runs for **1**, **2** and resolvated **2**. Noting that the plots of TGA/DTA of resolvated **2** almost assembled that of **1** though the loss of solvents occurred in slightly lower temperature region, and this is due to the fact that the crystals of resolvated **2** were finely cracked.

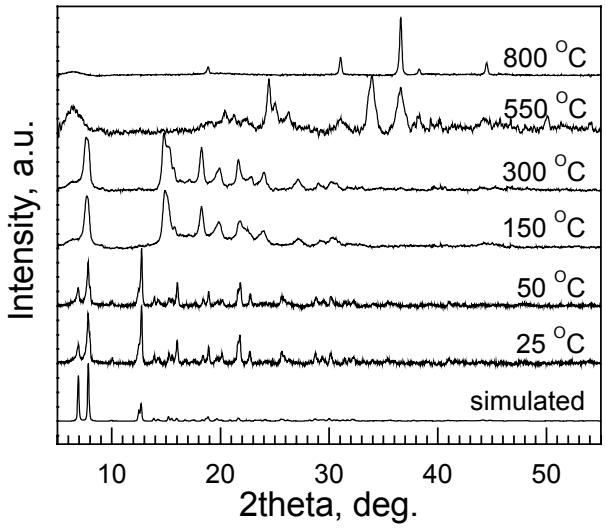

(a)

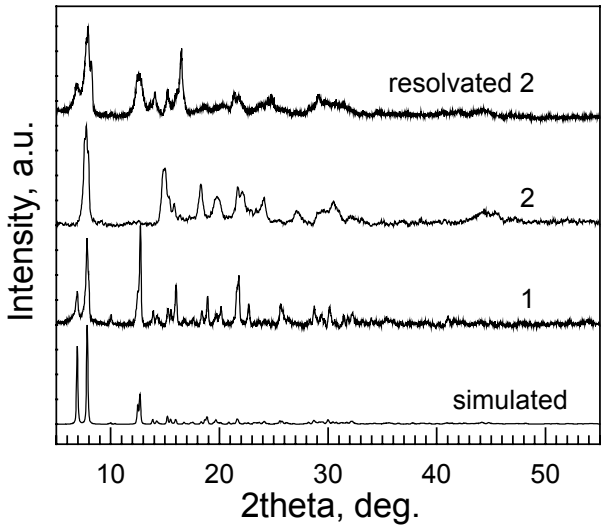

(b)

Fig. S3. (a) Temperature evolution of PXRD of **1** and (b) PXRD patterns for **1**, **2** and resolvated **2** (see text), with simulated one based on the single crystal structure of **1**.

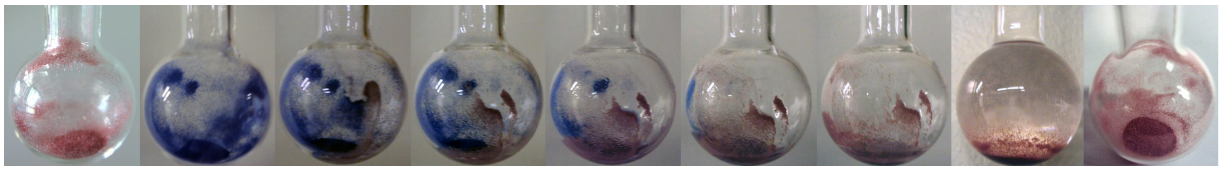

a b c d e f g h i

Fig. S4. The photos for resolvation procedure of **2**, (a) the as prepared sample of **1**, (b) the de-solvated phase, **2**, (c to h) the resolvation of **2** by adding water-ethanol solvents, and (i) the final dried resolvated **2**.

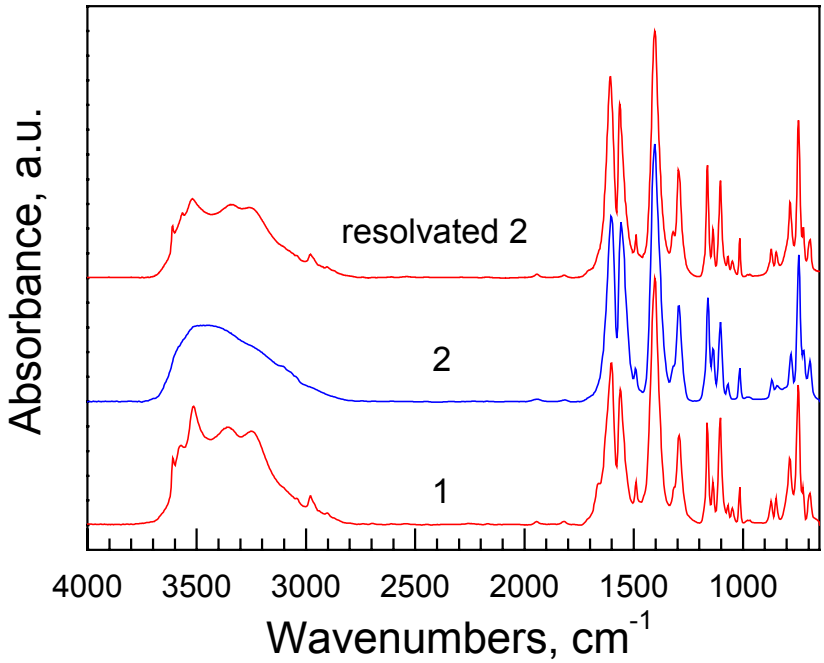

Fig. S5. Overlay of IR spectra of **1**, **2** and resolvated **2**, noting that the spectrum of resolvated **2** recovered the features of the spectrum of **1**.

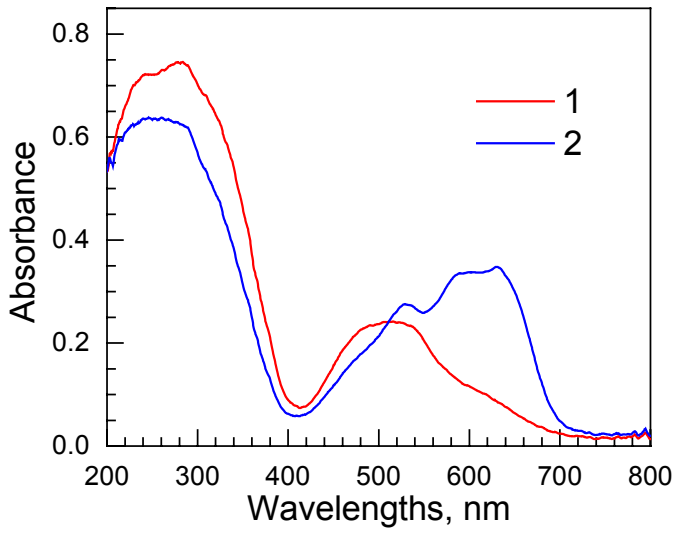

Fig. S6. UV-Vis spectra of **1** and **2**.

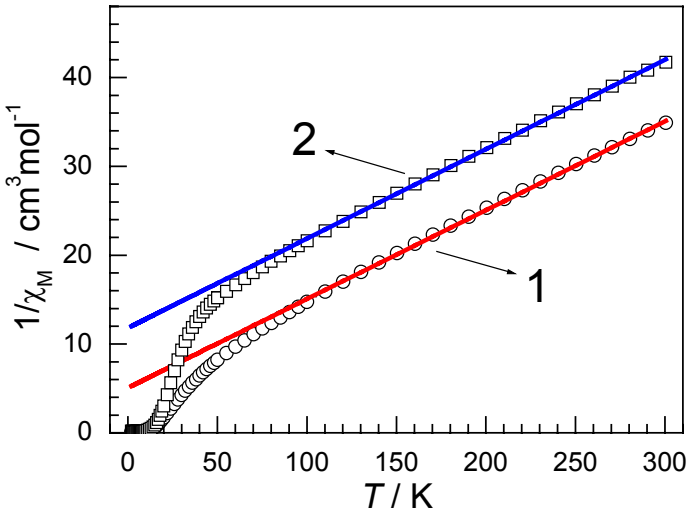

Fig. S7. The $1/\chi_M$ *vs* T plots for **1** and **2**, with the Curie-Weiss fittings in red lines.

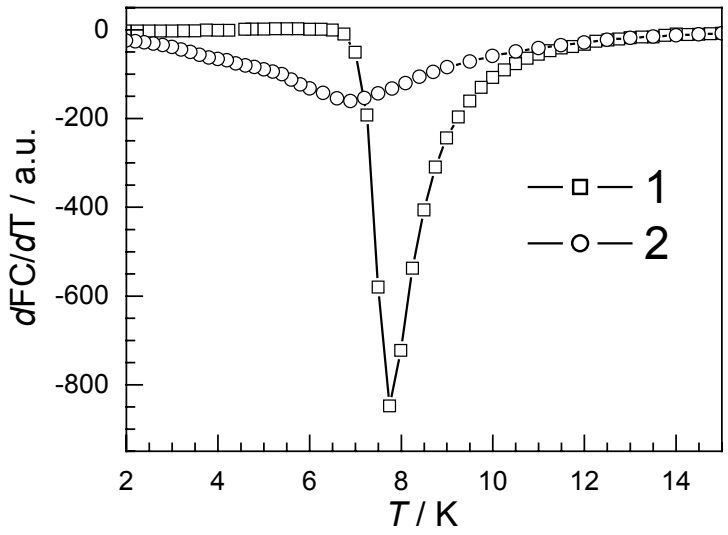

Fig. S8. *d*FC/d*T* plots of FC magnetization data for **1** and **2** under 20 Oe field.

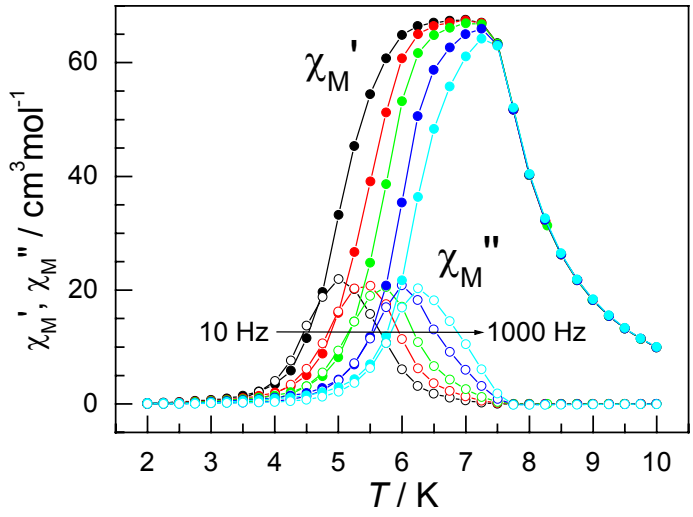

(a)

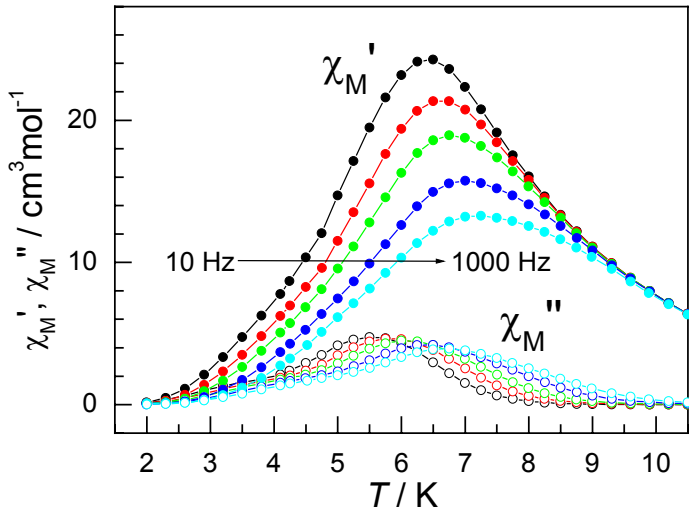

(b)

Fig. S9. Temperature dependence of ac susceptibilities of **1** (a) and **2** (b) under a zero Oe dc field in frequencies of 10, 36, 100, 360 and 1000 Hz.

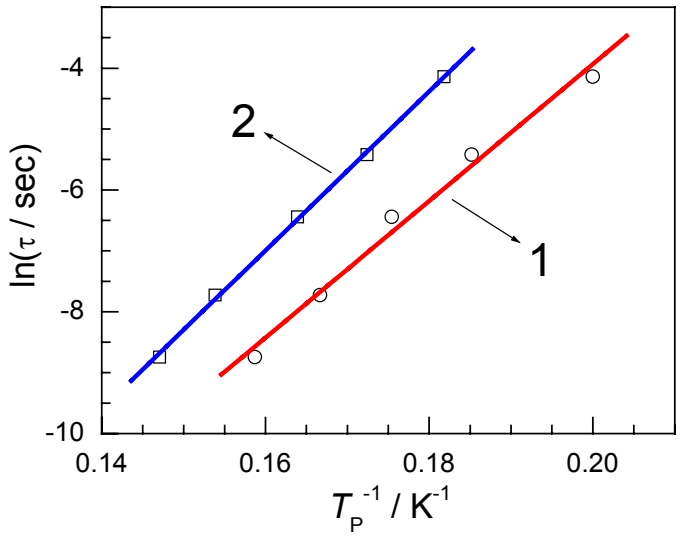

Fig. S10. The fitting plots of the Arrhenius law to frequency dependence of the χ_M" for **1** and **2**.